Fig. S1. Calcium requirement for dorsal closure. (A) Mosaicism due to expression of UAS-C2:GFP in the AS by c381-GAL4. Measurements for GFP signal at cell boundaries were taken for cells with neighbors that express lower levels of C2:GFP. Scale bar, 25 μm. (B) AS cells expressing mCD8:GFP during closure. Dashed white line denotes perimeter used for kymograph. (B') Kymograph of GFP signal along the traced boundary of an AS cell expressing mCD8:GFP (constitutive membrane localization) over time (3 s / frame). Scale bar, 10 μm. LUT (0-255 pixel values) is shown to the right of the kymograph. (C) Example data set used in cross correlation of normalized C2:GFP fluorescence signal and normalized change in perimeter for AS cells. Vertical lines correspond to local minima in C2:GFP ratio to visualize anti-phase relationship. (D) Embryo expressing mRFP labeled F-actin and GCaMP in the AS. A GFP flash (indicating increased Ca^{2+} levels) is shown (30 s). GFP signal in 0 and 180 s panels is due to autofluorescence of vitelline membrane. Quantification of spontaneous Ca^{2+} flashes for a single cell (D') in the group of AS cells (D'') that exhibit this behavior. Flash duration, time elapsed for GFP signal to return to baseline; % GFP change, relative change in intensity of GFP signal in the AS cell (averaged over apical area); time to recovery, time elapsed between peak GFP signal and when the AS apical area begins to increase again (stops contracting); % area change, apical area change over the time to recovery, as a percentage of apical area at the peak GFP signal. (E, E') Chelation of extracellular calcium via microinjection of BAPTA into the perivitelline space leads to closure failure in a dose-dependent manner. At lower doses of BAPTA closure is morphologically wildtype. Time in minutes; scale bar, 25 μm. (F) Chelation of calcium using a cell permeable chelator, NP EGTA AM, leads to dorsal closure failure in a dose-dependent manner. (F') Closure fails when the epithelial sheet loses integrity (arrowhead), which is preceded by disruption of actin structures, including the actomyosin purse string. Scale bar, 10 μm.

Fig. S2. MGC inhibition by $GdCl_3$ and early injection of GsMTx4. (A) 50mM $GdCl_3$ microinjection into dorsal closure staged embryos leads to epithelial disruption and failure to close. Scale bar, 20 μm. Time in minutes. Given the non-specific nature of $GdCl_3$ inhibition we cannot attribute these findings solely to the inhibition of MGCs. (B) Embryos control injected before germband retraction complete both germband retraction and closure. (C) Embryos microinjected with 5 mM tip concentration GsMTx4 before germband retraction fail to complete either retraction or closure. Failure of morphogenesis at or before closure is 92.5% penetrant (n = 27) at 5 mM GsMTx4 when embryos are microinjected during germband extension, compared to 0% (n = 15) in control injected embryos. Time in minutes; scale bar, 25 μm. Embryos express sGMCA for visualization of F-actin. (D) E-cadherin-GFP localizes to the cell membrane in AS cells. (E) E-cadherin-GFP puncta develop in the cytoplasm of AS cells in embryos treated with 5 mM GsMTx4. (F) Example of a cell-cell boundary in the AS of control (upper panel) and GsMTx4 treated (lower panel) embryos. GFP signal is lost from the cell-cell boundaries after GsMTx4 treatment. Scale bar (D, E) 10 μm.

Fig. S3. Knockdown of RPK or dTRPA1 expression during closure. (A) Western blot analysis of Ripped pocket (65kD) or (B) dTRPA1 (150kD) knockdown via RNAi. (A', B') Actin loading controls. Embryo lysate genotypes for (A, A') lane 1, tubulinGAL4>UAS-GFP-rpk; lane 2, w1118; lane 3, tubulinGAL4>UAS-*rpkRNAi*. Genotypes for (B, B') lane 1, sqhGAL4>UAS-trpA1 (approximately 100kD, see Rosenzweig et al., 2005); lane 2, w1118; lane 3, sqhGAL4>UAS-*trpA1 RNAi*. (C) Embryos of the genotype *w; engrailedGAL4 / UAS-GFP-moesin* complete closure. Expression of (D) *rpkRNAi* or (E) *trpA1RNAi* via *engrailedGAL4* results in closure that is morphologically indistinguishable from control. (F) Embryos homozygous for the $dtrpA1^{ins}$ mutation, expressing sGMCA, are morphologically indistinguishable from wildtype. (G) trpA1GAL4 drives weak expression of the UAS-actin-GFP reporter in the AS (arrowheads), most of which is obscured by autofluorescence from the yolk. (H) anti-dTRPA1 staining of w1118 embryos display low levels of ubiqiutous staining during dorsal closure stages. (I) Anti-RPK antibody recognizes apical puncta in AS cells. An XZ view of AS cells along the white dashed line shows RPK puncta approximately at the same plane as anti-phosphotyrosine (PY) staining, which labels apical cell-cell junctions. (J) Live image from a *rpk/Df* embryo expressing sGMCA. Apical actin networks (red arrows), junctional belts (yellow arrow) and purse string (white arrow) structures are observable. (K) c381-GAL4 driving UAS-*rpkRNAi* or (L) homozygous *Df/Df* embryos have reduced RPK staining (middle panels, red in merge). Phosphotyrosine staining (left panels, green in merge) labels cell-cell junctions. Scale bars, 25 μm in (C, K) 10 μm in (I).

Fig. S4. RNAi expressing embryos fail to recover from laser microsurgery. Embryos expressing (A) *rpkRNAi* or (B) *trpA1RNAi* in the amnioserosa are targeted for laser wounding (orange dashed line in top panels), and fail to complete wound healing. Time in minutes; scale bar, 25 μm.

Fig. S5. Model for channel activity in dorsal closure epithelia. Top two panels indicate the tissue depicted in the lower two panels. For a single cell (cell 1) a force (red arrow) is exerted on the MGCs in that cell either by external sources (*e.g.,* a neighboring cell) or the local activity of the contractile cytoskeleton. The applied force causes the MGCs to transition from closed (T_0, orange) to open (T_1, blue) allowing the influx of Ca^{2+} ions and leading to Ca^{2+}-dependent contractility.

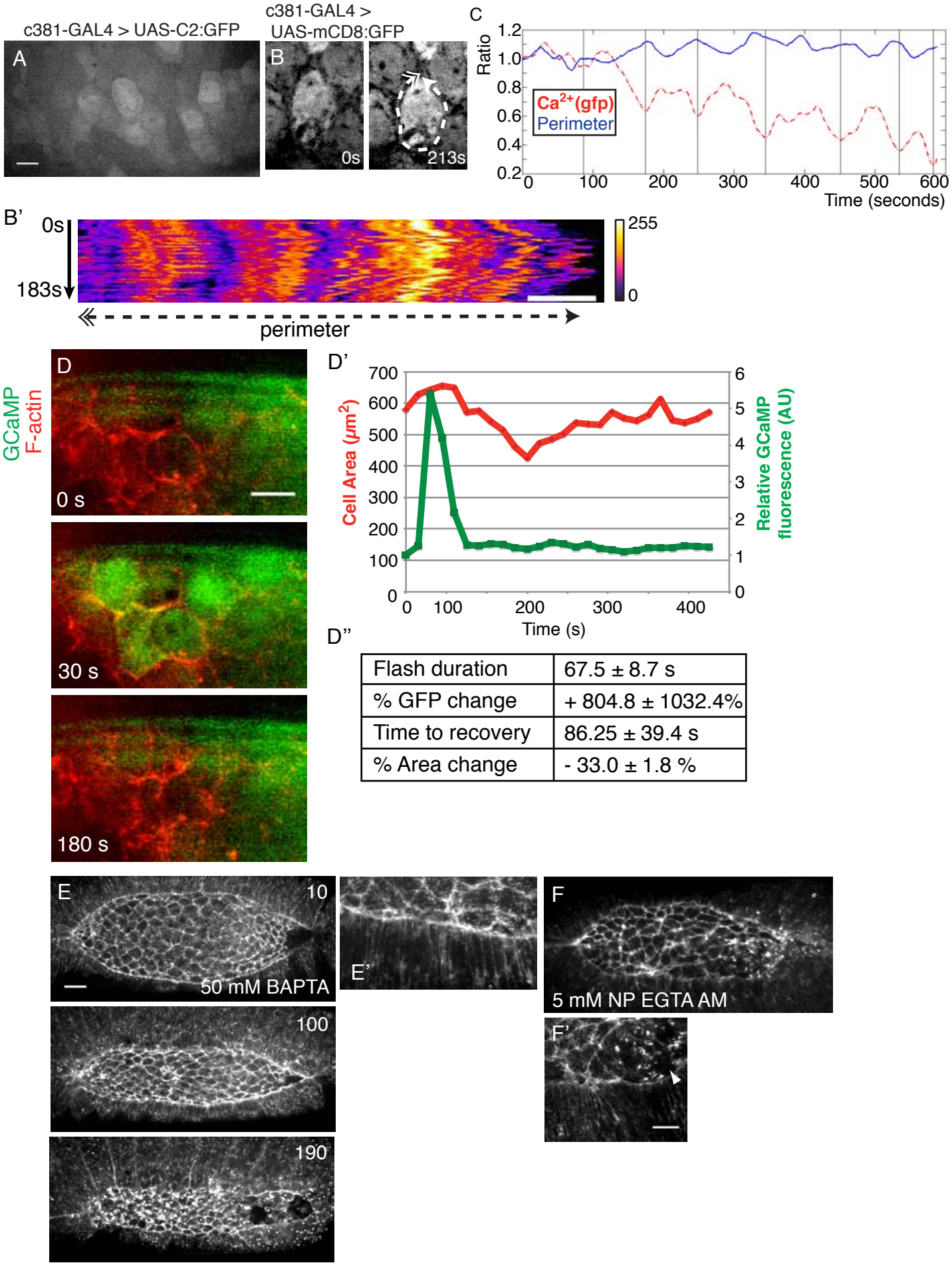
c381-GAL4 > UAS-C2:GFP
c381-GAL4 > UAS-mCD8:GFP
A
B
0s
213s
C
Ratio
1.2
1.0
0.8
0.6
0.4
0.2
Ca2+(gfp)
Perimeter
0
100
200
300
400
500
600
Time (seconds)
B'
0s
183s
255
0
perimeter
D
GCaMP
F-actin
0 s
30 s
180 s
D'
Cell Area (μm2)
Relative GCaMP fluorescence (AU)
700
600
500
400
300
200
100
0
6
5
4
3
2
1
0
0
100
200
300
400
Time (s)
D''
Flash duration
67.5 ± 8.7 s
% GFP change
+ 804.8 ± 1032.4%
Time to recovery
86.25 ± 39.4 s
% Area change
- 33.0 ± 1.8 %
E
10
50 mM BAPTA
100
190
E'
F
5 mM NP EGTA AM
F'

Figure S1

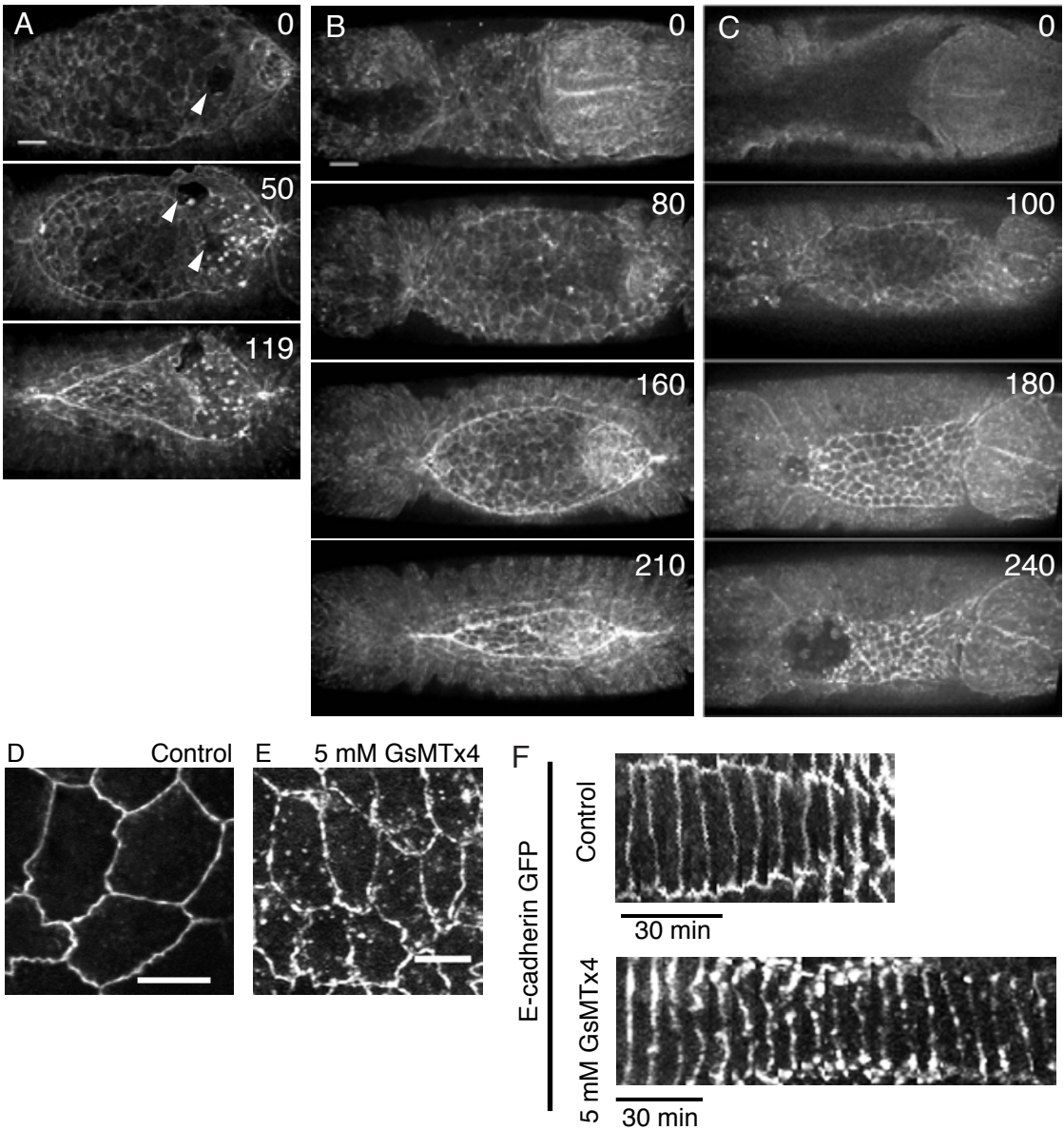
GdCl3
Control injected
5mM GsMTx4
A
0
50
119
B
0
80
160
210
C
0
100
180
240
D
Control
E
5 mM GsMTx4
F
E-cadherin GFP
Control
30 min
5 mM GsMTx4
30 min

FIGURE S2

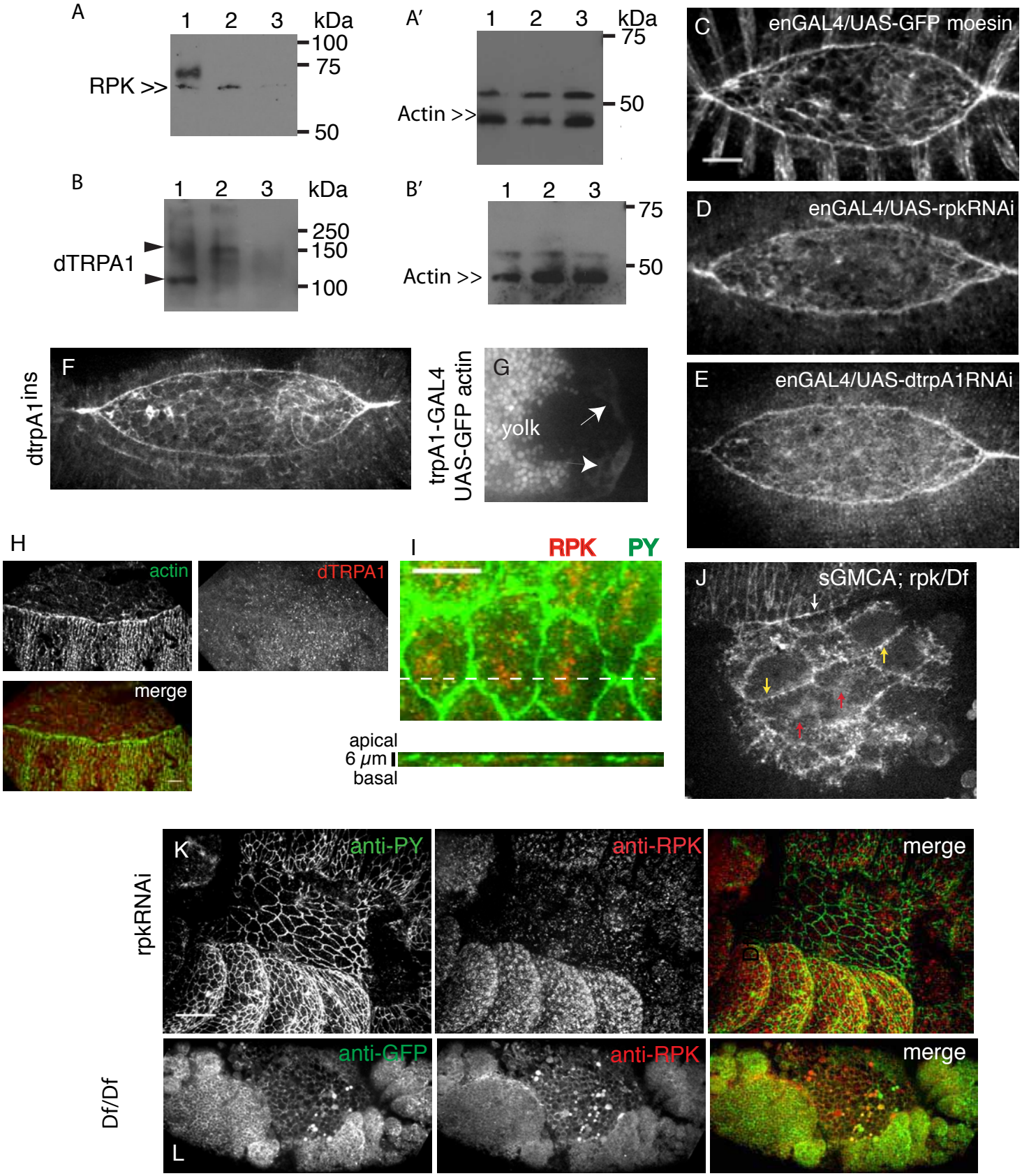
A
1 2 3 kDa
RPK >>
100
75
50
A′
1 2 3 kDa
Actin >>
75
50
B
1 2 3 kDa
dTRPA1
250
150
100
B′
1 2 3
Actin >>
75
50
C
enGAL4/UAS-GFP moesin
D
enGAL4/UAS-rpkRNAi
E
enGAL4/UAS-dtrpA1RNAi
F
dtrpA1ins
G
trpA1-GAL4
UAS-GFP actin
yolk
H
actin
dTRPA1
merge
I
RPK PY
apical
6 μm
basal
J
sGMCA; rpk/Df
rpkRNAi
K
anti-PY
anti-RPK
merge
Df/Df
L
anti-GFP
anti-RPK
merge

Figure S3

Fig. S4

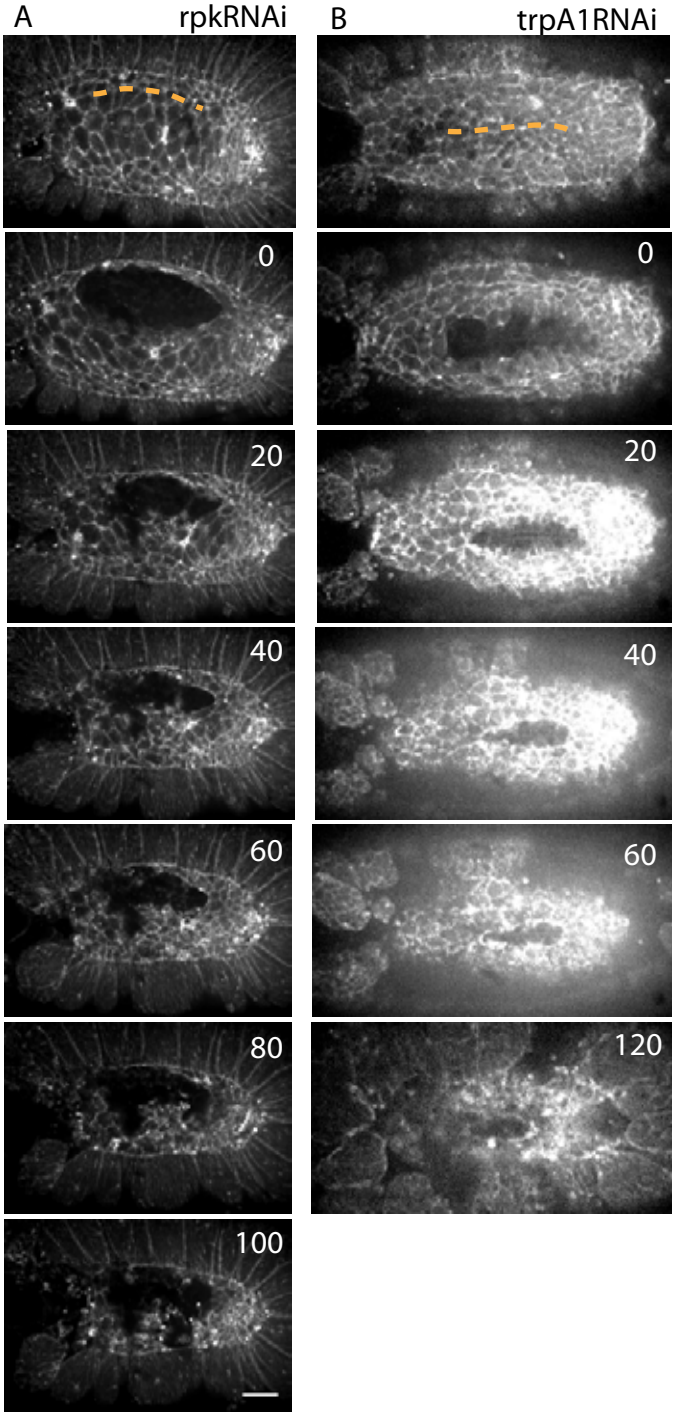

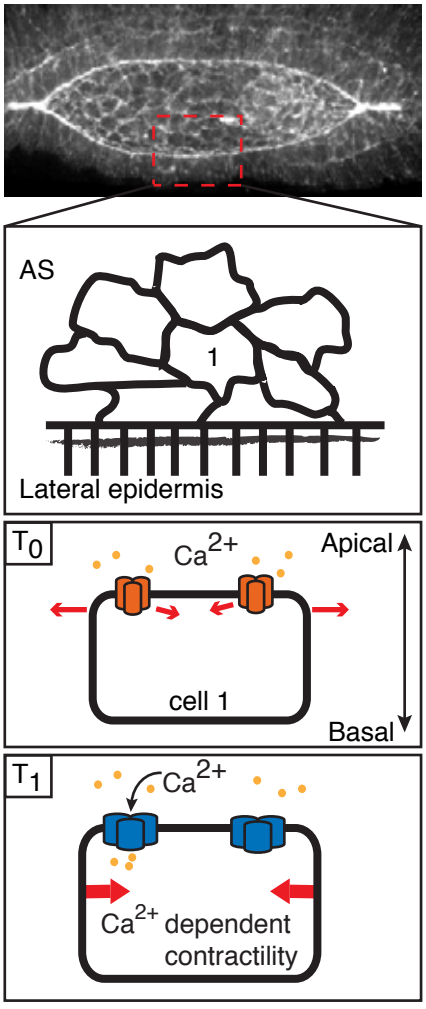
AS
1
Lateral epidermis
T0
Ca2+
Apical
cell 1
Basal
T1
Ca2+
Ca2+ dependent
contractility

Fig. S5

Movie 1. Amnioserosa apical cell contraction induced by uncaging of calcium. *w; c381GAL4, ubi-E-Cadherin-GFP / UAS-GCaMP3* embryo injected with 1 mM NP-EGTA AM. Uncaging recorded at 1 frame = 0.09 s (to avoid imaging artifacts from laser) and post-uncaging recorded at 1 frame = 60 s; the movie plays at a constant frames per second, thus the post-uncaging images will appear faster. Yellow line in time frame 1 (t =0) indicates beam path for uncaging. Movie 1 is the source of the micrograph in Figure 1B. Scale bar, 10 μm.

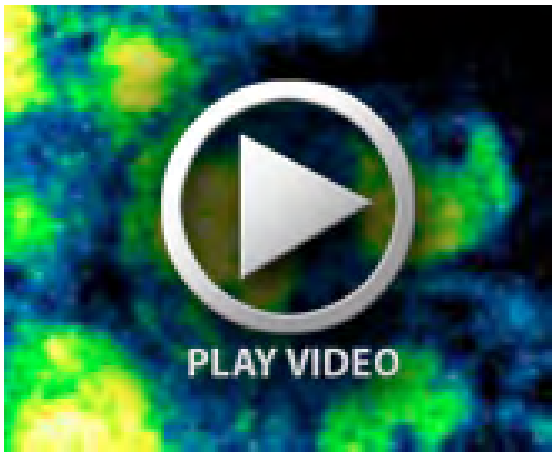

Movie 2. An example of C2:GFP dynamics in a contracting AS cell. Blue represents low levels of GFP signal, white/yellow represents high levels of GFP signal. 1 frame = 3 s. Movie 3 is the source of the micrograph in Figure 1E.

Movie 3. Acute effects of 10 mM GsMTx4 on the actomyosin structures and cell constriction of AS cells during closure. Time of microinjection is labeled in the upper left corner. Actin is visualized by sGMCA; 1 frame = 10 s. Movie 1 is the source of the micrograph in Figure 2A'. Scale bar, 10 μm.

Movie 4. Apical actomyosin network dynamics in the AS during dorsal closure. Apical actin networks are defined as the GFP signal (sGMCA) which transiently appears on the apical surface of most AS cells, as opposed to the stable signal observed at cell-cell junctions, Apical actin networks are visualized by sGMCA labeling F-actin; 1 frame = 30 s.

Table S1. Injection of calcium chelators inhibits dorsal closure.

Chelator	Tip concentration (mM)	N	% DC defects	% lethality
NP-EGTA AM	5	18	76.9	72.2
	1	13	69.2	30.8
	0.5	18	28.5	38.9
BAPTA	75	33	75.8	87.9
	50	43	34.4	74.4
	25	13	0	0
	10	16	0	0

Microinjection of the calcium chelator BAPTA into the perivitelline space of dorsal closure staged embryos blocks closure at high concentrations (≥ 50 mM, tip concentration). Microinjection of the cell permeable calcium chelator NP EGTA AM into staged embryos blocks dorsal closure in a dose-dependent manner.

Table S2 GsMTx4, an MGC inhibitor, blocks dorsal closure in a dose-dependent manner.

GsMTx-4 Tip Concentration (mM)	Range of Injected Volume (pL)	% Dorsal Closure Failure	N
20	137 - 143	88.9	9
5	77 – 356	51.6	31
2.5	127 – 248	34.6	26
1	239 – 244	23	12
0	40 – 893	0	16

GsMTx4 blocks dorsal closure in a dose-dependent manner. Microinjection of embryos at dorsal closure stages with a range of GsMTx4 concentrations led to dorsal closure defects.

Table S3. Gadolinium inhibits dorsal closure in a dose-dependent manner.

$GdCl_3$ Tip Concentration (mM)	Range of Injected Volume (pL)	N	Effects (% of total)			
			No effect	Abnormal Opening	Posterior holes, anterior zipping	Failure to close
100	277 – 588	20	15	15	5	65
50	180 – 507	15	13.3	13.3	60	13.3
25	190 – 245	13	30.8	15.4	46.2	7.6
20	241 – 840	18	44.4	22.2	33.3	0
10	190 – 1560	40	55	30	15	0
1	230 - 2157	16	56.3	43.7	0	0

$GdCl_3$ blocks dorsal closure in a dose-dependent manner. Microinjection of embryos at dorsal closure stages with a range of $GdCl_3$ concentrations led to dorsal closure defects.

Table S4. RNAi screen for candidate MGCs in dorsal closure

MGC Family	RNAi Target	Closure Defects	dh/dt (nm/s)	N (imaged)
TRP	TRP	-	5.5 ± 0.8	6
	Painless (TRPA)	-	5.1 ± 0.7	5
	TRPA1	+	n/a	
	Nanchung (TRPV)	-	5.6 ± 1.4	7
	Inactive (TRPV)	-	5.5 ± 0.8	8
	TRP-γ	-	6.8 ± 0.5	3
	TRPL	-	7.1 ± 1.3	4
	TRPM	-	6.4 ± 0.8	3
	nompC (TRPN)	-	5.2 ± 0.9	5
DEG/ENaC	Ripped pocket	+	n/a	
	Pickpocket	-	4.9 ± 1.0	6
	CG8546	-	5.3 ±1.2	5
	CG15555	-	6.2 ± 1.0	8
	CG13278	-	6.0 ± 1.4	6
	CG33289	-	6.1 ± 1.0	5
	Control	-	5.9 ± 0.9	7

Knockdown of candidate MGCs during dorsal closure. 15 genes encoding candidate channel subunits were targeted for RNAi knockdown. UAS-RNAi was driven using the MJ33a-GAL4, which expresses in the amnioserosa. Embryos were assayed for dorsal closure defects via confocal microscopy and time-lapse imaging of each genotype. Where possible, *dh/dt* was determined for each genotype and compared to controls. Knockdown that resulted in changes to dh/dt or observable morphological defects were tested further. For controls, we crossed sGMCA; MJ33a-GAL4 driver to sGMCA (III) stock.

Table S5. Knockdown of dTRPA1 or RPK expression is associated with embryonic lethality in Drosophila.

Embryonic Genotype	Embryonic Lethality	N	p
w1118	7.8 ± 3.8%	400	-
MJ33aGAL4 > UAS TRPA1 RNAi	42.0 ± 23.9%	514	0.03*
$trpA1^{1}$	12.0 ± 6.5%	361	0.31
$trpA1^{ins}$	26.6 ± 19.3%	525	0.1
$trpA1^{ins}$, MJ33aGAL4/ $trpA1^{ins}$, UAS TRPA1 RNAi	8.7 ± 7.8%	208	0.83
MJ33aGAL4 > UAS RPK RNAi	69. 5 ± 15%	462	0.0002*
Rpk^{53} (M+/Z-)	20.2 ± 13.6%	402	0.1
Rpk^{53} (M-/Z+)	33.7 ± 6.4%	210	0.004*
Rpk^{53} (M-/Z-)	34.0 ± 9.4%	159	0.002*
Rpk^{53}/Df(3R)ED5092 (M-/Z-)	43.4 ± 6.2%	407	< 0.0001*
$Rpk^{EY12268}$	29.5 ± 5.4%	317	0.0006*

Knockdown of dTRPA1 or RPK expression is associated with embryonic lethality in Drosophila. * = statistically significant p values, compared to w1118 embryonic lethality.